Photolysis of Sulfur Dioxide in the Presence of Foreign Gases. I. Carbon Monoxide and Perfluoroethylene[1a]

Edwin Cehelnik,[1b] Chester W. Spicer,[1b] and Julian Heicklen*

Contribution from the Department of Chemistry and
Center for Air Environment Studies, The Pennsylvania State University,
University Park, Pennsylvania 16802. *Received April 17, 1970*

Abstract: SO_2 was photolyzed in the presence of CO and C_2F_4 at room temperature with 3130-Å radiation. With CO the initial products were CO_2 and polymer. Carbonyl sulfide was produced as a secondary product. The CO_2 quantum yield, $\Phi\{CO_2\}$, was independent of irradiation time, nearly independent of the absorbed intensity, I_a, and independent of SO_2 pressure for SO_2 pressures in excess of about 60 Torr. $\Phi\{CO_2\}$ increased with increasing CO pressure and with decreasing SO_2 pressure for SO_2 pressures below 60 Torr. The addition of NO, biacetyl, or O_2 inhibited product formation, but did not reduce it to zero. The addition of excess N_2 had no effect at large CO pressures, but reduced $\Phi\{CO_2\}$ about 60% at low CO and SO_2 pressures. With C_2F_4 the products were CF_2O, c-C_3F_6, and polymer. $\Phi\{CF_2O\}$ was nearly constant at 0.05 for all runs with C_2F_4 pressures greater than 20 Torr. At low C_2F_4 pressures, $\Phi\{CF_2O\}$ fell as $[C_2F_4]$ was reduced or $[SO_2]$ was increased from 2 to 75 Torr. At higher SO_2 pressures, no change was observed. $\Phi\{c\text{-}C_3F_6\}$ was always less than $\Phi\{CF_2O\}$ but increased as the C_2F_4 pressure was raised. The addition of NO suppressed, but did not eliminate, product formation. The addition of excess N_2 had no effect. The results cannot be understood in terms of only the two known luminescing states. They are interpreted in terms of four electronically excited states of SO_2, two singlet states, and two triplet states. A complete mechanism is proposed which is consistent with emission and other photochemical studies, and the relative rate constants are obtained.

The primary photophysical processes in SO_2 when excited into the absorption band centered at about 3000 Å have been studied in detail for about a decade. These studies include the excellent work of Duncan and his coworkers,[2] Strickler and Howell,[3] Mettee,[4-6] and Calvert and his coworkers.[7-10] The details of the primary process have been elucidated through lifetime measurements of emission, fluorescence and phosphorescence yields during steady-state exposure, and by biacetyl sensitization. The mechanism resulting from these studies is

$$^1SO_2 + SO_2 \longrightarrow 2SO_2 \qquad (1a)$$

$$\longrightarrow {}^3SO_2 + SO_2 \qquad (1b)$$

$$^1SO_2 \longrightarrow SO_2 + h\nu_f \qquad (2a)$$

$$\longrightarrow SO_2 \qquad (2b)$$

$$\longrightarrow {}^3SO_2 \qquad (2c)$$

$$^3SO_2 \longrightarrow SO_2 + h\nu_p \qquad (3a)$$

$$\longrightarrow SO_2 \qquad (3b)$$

$$^3SO_2 + SO_2 \longrightarrow 2SO_2 \qquad (4a)$$

$$\longrightarrow SO_3 + SO \qquad (4b)$$

where the superscripts 1 and 3 refer to an excited singlet and triplet state, respectively. Rate constants have been determined for all the steps.

Furthermore, Thrush and his coworkers[11-16] studied the emission of SO_2 produced from the reactions of SO with O_3 or oxygen atoms. Their results are consistent with the above mechanism except for minor discrepancies.[17]

Electronically excited SO_2 is also known to react with O_2 to produce SO_3, though the quantum yield is small and the details of the process are not known.[18,19]

Dainton and Ivin[20,21] studied the photolysis of SO_2 in the presence of several paraffin and olefin hydrocarbons. The principal products were sulfinic acids. The quantum yields were independent of SO_2 pressure, but increased with the hydrocarbon pressure to a maximum value of about 0.35. A negative temperature coefficient was found between 15 and 100°.

More recently, Timmons[22] has reexamined the photolysis of SO_2 in the presence of alkanes. For isobutane as the added gas, he found that for an SO_2 pressure of 20 Torr, the total quantum yield first increased with isobutane pressure and then became constant at ~0.090 for isobutane pressures above 200 Torr. The addition of excess methane had almost no effect on the quantum yield. The negative temperature coefficient reported by Dainton and Ivin was confirmed.

---

(1) (a) CAES Publication No. 156-70; (b) U. S. Public Health Service Air Pollution Trainee.

(2) (a) K. F. Greenough and A. B. F. Duncan, *J. Amer. Chem. Soc.*, **83**, 555 (1961); (b) R. B. Caton and A. B. F. Duncan, *ibid.*, **90**, 1945 (1968).

(3) S. J. Strickler and D. B. Howell, *J. Chem. Phys.*, **49**, 1947 (1968).

(4) H. D. Mettee, *ibid.*, **49**, 1784 (1968).

(5) H. D. Mettee, *J. Amer. Chem. Soc.*, **90**, 2972 (1968).

(6) H. D. Mettee, *J. Phys. Chem.*, **73**, 1071 (1969).

(7) T. N. Rao, S. S. Collier, and J. G. Calvert, *J. Amer. Chem. Soc.*, **91**, 1609 (1969).

(8) T. N. Rao, S. S. Collier, and J. G. Calvert, *ibid.*, **91**, 1616 (1969).

(9) S. Okuda, T. N. Rao, D. H. Slater, and J. G. Calvert, *J. Phys. Chem.*, **73**, 4412 (1969).

(10) S. S. Collier, A. Morikawa, D. H. Slater, J. G. Calvert, G. Reinhardt, and E. Damon, *J. Amer. Chem. Soc.*, **92**, 217 (1970).

(11) C. J. Halstead and B. A. Thrush, *Chem. Commun.*, 213 (1965).

(12) C. J. Halstead and B. A. Thrush, *Photochem. Photobiol.*, **4**, 1007 (1965).

(13) C. J. Halstead and B. A. Thrush, *Proc. Roy. Soc., Ser. A*, **295**, 363 (1966).

(14) C. J. Halstead and B. A. Thrush, *ibid., Ser. A*, **295**, 380 (1966).

(15) B. A. Thrush, C. J. Halstead, and A. McKenzie, *J. Phys. Chem.*, **72**, 3711 (1968).

(16) A. McKenzie and B. A. Thrush, *Proc. Roy. Soc., Ser. A*, **308**, 133 (1968).

(17) N. Cohen and J. Heicklen, "Comprehensive Chemical Kinetics," Vol. 6, Elsevier, Amsterdam, in press.

(18) P. A. Leighton, "Photochemistry of Air Pollution," Academic Press, New York, N. Y., 1961, p 236.

(19) D. S. Sethi, E. R. Allen, and R. D. Cadle, Fifth International Conference on Photochemistry, Yorktown Heights, N. Y., 1969.

(20) F. S. Dainton and K. J. Ivin, *Trans. Faraday Soc.*, **46**, 374 (1950).

(21) F. S. Dainton and K. J. Ivin, *ibid.*, **46**, 382 (1950).

(22) R. B. Timmons, *Photochem. Photobiol.*, **12**, 219 (1970).

Timmons[22] also made a limited study of the photolysis of SO_2 in the presence of CO. For four runs at 25° and $[SO_2] = 20$ Torr, he found that CO_2 was produced with a quantum yield increasing from 5.2×10^{-3} at 21 Torr of CO to 7.4×10^{-3} at 420 Torr of CO. A negative temperature coefficient was also found for this reaction.

In our laboratory we have initiated a program to study the chemical reactions of electronically excited SO_2. In this paper we report some results with CO and C_2F_4.

Experimental Section

Materials. Matheson Co. SO_2 (anhydrous), NO (Technical), O_2 (extra dry), N_2 (prepurified), and CO (CP) were used. The O_2 and N_2 were used as received (the only significant impurities were 0.05% N_2 and 0.07% O_2, respectively), but the other gases were further purified. The SO_2 was distilled at −98° and the fraction volatile at −98° but condensable at −130° was used. It contained about 0.5% CS_2 and 0.1% H_2S as the only impurities. For NO the fraction volatile at −186° was used after degassing at −196°. For the early runs, the CO was passed slowly through 25 ft of $^3/_{16}$-in. diameter copper tubing immersed in liquid nitrogen to remove most of the CO_2 and iron carbonyl. After purification, the CO contained about 0.001% CO_2. For later runs a 4-ft, $^1/_4$-in. diameter copper tube containing Lithosorb was incorporated before the other column to further reduce the CO_2 impurity to undetectable values (~2 ppm).

Eastman Organic Chemical biacetyl was used after degassing at −80°. C_2F_4 and CF_3I were obtained from Peninsular Chem-Research Co. For C_2F_4 the fraction volatile at −130° but condensable at −196° was used; no impurities could be detected. For CF_3I the fraction between −130 and −160° was used for early runs. It contained measurable CO_2. For later runs the CF_3I was passed through 1 ft of Ascarite and degassed at −196°. The CO_2 impurity was reduced to 4 ppm, which was negligible.

Procedure. Irradiations were done in cyclindrical quartz cells 10 cm long by 5 cm in diameter. The radiation was from a medium-pressure mercury arc and passed through a Corning 0-54 filter before entering the reaction vessel. This filter removed radiation below 3000 Å and transmitted about 1% at 3020 Å and 35% at 3130 Å.

For the SO_2–CO photolyses, a Hanovia medium-pressure mercury U-tube lamp, Type 30620, was used. The only product measured was CO_2, which was determined by gas chromotgraphy initially using a 4-ft by $^1/_4$-in. Porapak T column at 0° with a He flow rate of 200 cm³/min in conjunction with a Gow-Mac thermistor detector. For later runs the column length was reduced to 1 ft and the He flow rate to 100 cm³/min. A dark run accompanied each photolysis; the background CO_2 was always constant for a given CO pressure and less than 10% (usually ≃5%) of that in the irradiated sample. This background value was subtracted to compute quantum yields.

For the SO_2–C_2F_4 photolyses, either a Hanovia 200-W medium-pressure Type 654A36 mercury arc or a Hanovia 100-W medium-pressure U-tube Type SH lamp was used. The radiation passed through the cell perpendicular to the cell axis. The cell was fitted with NaCl windows and situated in the sample beam of a Beckman IR-10 infrared spectrometer for continual analysis of CF_2O at 5.12 μ. For the runs at low pressures of C_2F_4 and all the runs with 2 Torr of SO_2, scale expansion was used. Corrections for the background bands of C_2F_4 and NO were made. After irradiation was terminated, the gases were collected and passed into a Varian Aerograph No. 1520 chromatograph utilizing a 10-ft, $^1/_4$-in. Porapak Q column at 45° with a He flow rate of 30 cm³/min. A thermal conductivity cell operating at 95° with a current of 250 mA served as a detector. The only product found (in addition to the CF_2O) was c-C_3F_6, which was calibrated from authentic samples of c-C_3F_6 produced from the mercury-sensitized photolysis of C_2F_4.

Actinometry. To measure the absorbed intensity, I_a, CF_3I was photolyzed in the presence of O_2, where $\Phi\{CF_2O\}$ is assumed to be unity.[23] The quantum yield of unity at room temperature was confirmed by comparison with the photolysis of acetone at 142°, where $\Phi\{CO\}$ is known to be one. The CF_2O was measured either directly by infrared analysis or by converting it to CO_2 and using gas chromatography. In the latter method, corrections were made for background CO_2. To eliminate possible geometrical corrections, I_a was measured for matched absorbances of SO_2 and CF_3I.

Results

SO_2–CO System. In the photolysis of SO_2 in the presence of CO, the products of the reaction are CO_2, OCS, and polymer both in the absence and presence of NO, biacetyl, or O_2. With O_2 present the polymer production is inhibited, and none is formed if excess O_2 is present. Carbonyl sulfide is a secondary product and its quantum yield extrapolates to zero at zero exposure time.

To check that longer wavelengths were not participating in the photochemistry, some runs were done with a Corning O-52 filter to eliminate 3130- and the weak 3340-Å radiation, but not 3660-Å radiation. For such irradiations, no products could be found for the low absorbed intensities used in this study. The CO_2 quantum yields are listed in Table I for photolysis of SO_2–CO mixtures with radiation principally at 3130-Å. $\Phi\{CO_2\}$ is independent of the duration of irradiation and the SO_2 pressure, but increases with [CO]. These results are shown graphically in Figure 1, where it can be seen that $\Phi\{CO_2\} = 1.87 \times 10^{-5}[CO]$. The effect of absorbed intensity is illustrated in Figure 2. At reduced intensities $\Phi\{CO_2\}$ is slightly diminished, but this may reflect experimental uncertainty. A factor of 10 reduction in I_a only reduces $\Phi\{CO_2\}$ by about 25%. We do not consider this reduction meaningful owing to the background CO_2 correction in the actinometry which sometimes amounted to 30%.

Table I. Photolysis of SO_2 in the Presence of CO at 3130 Å and Room Temperature (Early Runs)

[CO], Torr	$[SO_2]$, Torr	I_a, μ/min	Irradiation time, min	$10^4\Phi\{CO_2\}$
20	30.5	87.5	150.0	3.82
52	31	102	306.0	13.1
79	92	102	210.0	15.0
102	31	87.5	240.0	20.0
116	75	102	155.0	19.5
185	31	102	180.0	33.6
201	304	102	90.0	40.0
202	423	102	180.0	42.5
222	75	102	90.0	38.0
246	75	102	155.0	43.1
274	30	87.5	135.0	49.5
289	31	87.5	165.0	49.0
307	31	102	165.0	55.8
334	31	87.5	105.0	60.7
351	74.5	102	90.0	62.0
394	30.5	18.8	295.0	54.3
401	31	40.3	180.0	64.7
404	76	102	106.0	63.5
417	31	127	30.0	72.0
429	31	11.8	410.0	56.0
438	100	102	120.5	83.3
448	31	102	60.0	80.8
454	30	97.5	180.0	85.1
456	30	79.3	60.0	84.5
465	30.5	97.5	61.0	87.2

Table II shows the effect of added biacetyl. The addition of biacetyl first reduces $\Phi\{CO_2\}$, but as large amounts of biacetyl are added $\Phi\{CO_2\}$ starts to rise again.

---

[23] J. Heicklen, *Advan. Photochem.*, 7, 57 (1969).

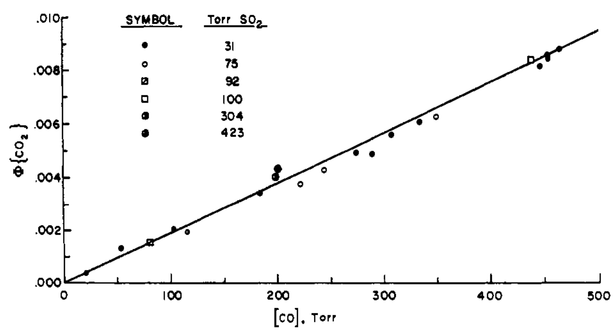

Figure 1. Plot of $\Phi\{CO_2\}$ *vs.* CO pressure in the photolysis of SO_2–CO mixtures at 3130 Å and room temperature; early runs at full intensity.

Table II. Photolysis of SO_2 in the Presence of CO and Biacetyl at 3130 Å and Room Temperature

[BiA], Torr	[CO], Torr	[SO_2], Torr	I_a, μ/min	Irradiation time, min	$10^4 \cdot \Phi\{CO_2\}$
0.3	351	76	85	130.0	53.8
0.55	420	32	77.5	75.0	62.4
0.7	351	78	85	123.0	41.3
1.18	415	32	77.5	120.0	41.5
2	300	360	105	241.0	19.9
2	412	32	77.5	265.0	25.3
3	419	31	77.5	200.0	23.8
4	350	76	85	245.0	18.4
4	350	76	85	300.0	18.9
4	237	190	105	245.0	10.8
6	255	316	105	325.0	10.1
10.5	416	33	77.5	145.0	22.0
16	413	33	127	30.0	24.0

This rise might be due to direct absorption of the 3130-Å radiation by the biacetyl, and we discount these results. Of course the biacetyl is a strong absorber of longer wavelength radiation which is also incident on the cell cell (*i.e.*, 3660, 4047, and 4358 Å). However, these wavelengths have no effect since mixtures of 7 Torr of biacetyl, 75 Torr of SO_2, and 180 or 325 Torr of CO irradiated through a Corning 0-52 filter (which transmits 3660 Å and above, but eliminates shorter wavelengths) produced no CO_2.

The effect of added NO is shown in Table III. Increasing the NO pressures reduces $\Phi\{CO_2\}$, but only to a limiting value about 0.13 that in the absence of NO. Irradiation of a mixture of 3.55 Torr of NO, 75 Torr of SO_2, and 390 Torr of CO produced no measurable amount of NO_2 ($\geq 100\ \mu$) as determined from absorption spectroscopy between 4000 and 4300 Å. Likewise, even when CO was absent and the NO pressure was in large excess (75 Torr of SO_2, 300 Torr of NO), NO_2 could not be detected.

Table III. Photolysis of SO_2 in the Presence of CO and NO at 3130 Å and Room Temperature

[NO], Torr	[CO], Torr	[SO_2], Torr	I_a, μ/min	Irradiation time, min	$10^4 \cdot \Phi\{CO_2\}$
0.230	389	77	151	120.0	51.6
0.580	448	12	52.6	230.0	38.8
0.620	396	76	151	115.0	36.1
1.35	423	44	120	120.0	23.2
1.40	394	75	151	120.0	22.1
2.15	389	75	151	100.0	17.5
3.55	390	75	151	90.0	11.0
5.80	337	136	175	300.0	10.2
6.0	423	11	52.6	315.0	11.2
6.13	391	75	151	250.0	10.7
9.00	395	76	151	360.0	9.75

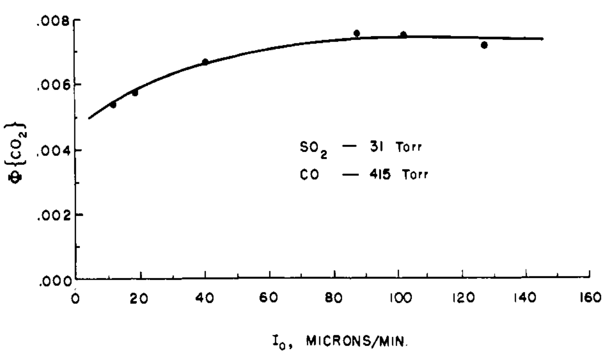

Figure 2. Plot of $\Phi\{CO_2\}$ *vs.* I_a in the photolysis of SO_2–CO mixtures at 3130 Å and room temperature; early runs, [SO_2] $\simeq$ 31 Torr, [CO] $\simeq$ 415 Torr.

The addition of O_2 also reduces $\Phi\{CO_2\}$, as shown in Table IV. However, the inhibition is not very marked.

Table IV. Photolysis of SO_2 in the Presence of CO and O_2 at 3130 A and Room Temperature

[O_2], Torr	[CO], Torr	[SO_2], Torr	I_a, μ/min	Irradiation time, min	$10^4 \cdot \Phi\{CO_2\}$
0.590	393	77	161	130.0	92.5
0.60	383	77	161	61.0	69.5
1.85	388	77	161	60.0	70.2
6.10	390	77	161	60.0	68.4
20	319	135	121	122.0	55.3
22	434	12	50	255.0	73.1
25	369	76	161	105.0	54.7
34	424	12	50	120.0	67.8
36	310	135	179	245.0	49.2
37	306	134	179	60.0	43.7

The partial quenching of CO_2 formation when biacetyl or NO is added shows that both singlet and triplet states of SO_2 participate in the production of CO_2. However, the results are contrary to that expected from the emission studies. If the reactions of CO with $^1SO_2$ and $^3SO_2$ are added to the mechanism consisting of reactions 1–4, then $\Phi\{CO_2\}$ should either depend on [SO_2] or be independent of [CO].

The above findings were sent to Professor Jack Calvert at Ohio State University, who, with George Jackson had initiated a study of the SO_2–CO reaction when the $^3SO_2$ is produced directly by absorption of radiation at 3530–3970 Å. Their room-temperature studies were at very much higher intensities, but at reactant pressures similar to those used by us: [SO_2], 58.3–145.2 Torr; [CO], 160–606 Torr; and [SO_2]/[CO], 0.096–0.908.[24] As expected from the emission mechanism, but contrary to our results, they found that $\Phi\{CO_2\}$ depended on the [SO_2] to [CO] ratio. Furthermore, they found a positive temperature coefficient for CO_2 production, whereas Timmons,[22] who excited SO_2 with 3130-Å radiation, found a negative temperature coefficient.

(24) G. E. Jackson and J. G. Calvert, private communication, 1970.

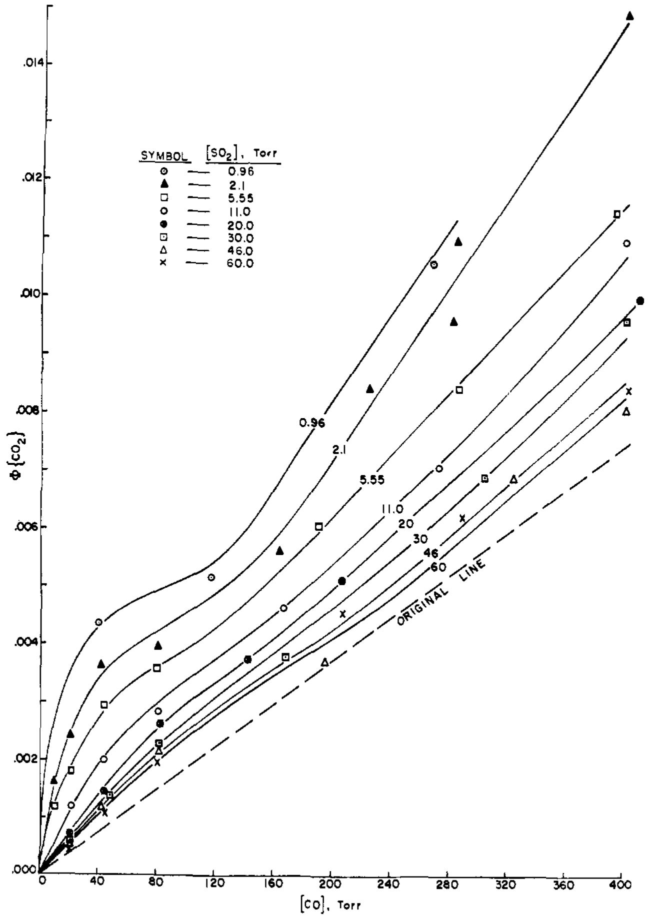

Figure 3. Plots of $\Phi\{CO_2\}$ *vs.* CO pressure in the photolysis of SO_2–CO mixtures at 3130 Å and room temperature for various SO_2 pressures; later runs at full intensity. The dotted line represents the results of the early runs as taken from Figure 1.

At the same time as the Jackson and Calvert experiments were in progress, we extended our work to lower SO_2 pressures. The results are listed in Table V. Three runs were done with 20 Torr of SO_2 and 44 Torr of CO, but for various exposure times; $\Phi\{CO_2\}$ was the same in all runs. The effect of absorbed intensity was studied for some runs at 2.1 Torr of SO_2 and 280–400 Torr of CO. A slight, but not meaningful drop in $\Phi\{CO_2\}$ was noticed as I_a was lowered by a factor of 5.4. The effects of both CO and SO_2 pressures were complex and are shown graphically in Figure 3. This figure contains plots of $\Phi\{CO_2\}$ *vs.* [CO] at various SO_2 pressures. The plot from Figure 1, which corresponds to high SO_2 pressures, is shown as the dotted line. Values of $\Phi\{CO_2\}$ obtained in the later runs are slightly higher than those obtained in the earlier runs for comparable reactant pressures. In the later work, the CO and the CF_3I actinometer were more thoroughly purified, the background concentrations for CO_2 were smaller, and the results should be more accurate. At all pressures of SO_2, $\Phi\{CO_2\}$ increases with [CO], but the constant [SO_2] curves lie higher as [SO_2] is reduced. For low [SO_2] and low [CO], the curves show a pronounced bump.

Table V. Photolysis of SO_2 in the Presence of CO at 3130 A and Room Temperature (Later Runs)

[CO], Torr	I_a, μ/min	Irradiation time, min	$10^4 \cdot \Phi\{CO_2\}$
	[SO_2] = 0.96 Torr		
40.5	3.75	262.0	43.6
117	3.75	163.0	51.7
286	3.75	165.0	107
	[SO_2] = 2.1 Torr		
10	7.54	593.0	16.3
21	7.54	270.0	24.2
42	7.54	153.0	36.3
81	7.54	155.0	39.8
164	7.63	410.0	56.3
225	7.63	90.0	84.5
281	7.63	120.0	96
283	7.87	100.0	110
283	1.43	427.0	90
302	7.54	130.0	101
352	1.43	280.0	92
400	7.63	70.0	150
	[SO_2] = 5.55 Torr		
10	20.0	333.0	10.4
21	20.0	200.0	17.7
44	20.0	215.0	29.4
80	20.0	200.0	35.8
190	22.0	120.0	60
285	22.0	50.0	84
392	22.0	100.0	115
	[SO_2] = 11.0 Torr		
22	41.7	100.0	11.7
44	41.7	100.0	19.9
81	41.7	100.0	28.4
166	44.1	46.0	46.6
272	44.1	25.0	70.8
399	44.1	21.0	110
	[SO_2] = 20 Torr		
20	68.6	180.0	7.4
44	71.0	62.0	14.5
44	71.0	120.0	14.2
44	71.0	240.0	13.8
82	68.6	60.0	26.6
142	71.0	180.0	37.6
206	71.0	60.0	51.2
410	71.0	55.0	100
	[SO_2] = 30 Torr		
20	85.6	200.0	6.6
47	85.6	95.0	14.0
82	85.6	90.0	22.9
168	94.7	30.0	38.0
302	94.7	25.0	68.9
399	94.7	30.0	98.3
	[SO_2] = 46 Torr		
20	109	185.0	6.6
42	109	45.0	12.0
82	109	30.0	22.2
195	123	45.0	37.2
323	123	20.0	69.0
400	123	20.0	90.5
	[SO_2] = 60 Torr		
20	130	123.0	5.8
44	130	80.0	10.8
81	130	30.0	19.5
207	138	25.0	45.4
308	138	50.0	62.2
405	138	25.0	84.8

The effect of additives on experiments with SO_2 pressures of 2.1 Torr is shown in Table VI. When 6 Torr or more of NO is added, $\Phi\{CO_2\}$ drops to about one-half its value in the absence of NO at any CO pressure. Thus singlet and triplet states are about equally important. Nitrogen, which effectively quenches both fluorescence and phosphorescence,[6] has no effect at all when about 300 Torr of CO is present. With about 44 Torr of CO, the addition of N_2 reduces $\Phi\{CO_2\}$ by about 60%.

Table VI. Photolysis of SO_2 in the Presence of CO and Other Gases[a]

[CO], Torr	[X], Torr	Irradiation time, min	$10^4\Phi\{CO_2\}$
		X = N_2	
42	0.0	153.0	36.3
46	108	256.0	17.5
44	407	250.0	15.6
302	0.0	130.0	101
302	86	295.0	107
303	461	264.0	105
299	493	248.0	116
		X = NO	
42	0.0	153.0	36.3
49	6.0	540.0	18.7
81	0.0	155.0	39.8
87	7.0	368.0	26.4
81	16.0	585.0	~35
164	0.0	410.0	56.3
170	7.0	240.0	46.5
184	7.0	260.0	42.4
281	0.0	120.0	95.8
314	7.0	235.0	57.8
312	8.0	428.0	~42
311	13.0	422.0	59.2
400	0.0	70.0	150
391	7.0	155.0	92

[a] $[SO_2] = 2.1$ Torr, $I_a = 7.8 \pm 0.3$ μ/min.

SO_2–C_2F_4 System. In the photolysis of SO_2–C_2F_4 mixtures the products are CF_2O, c-C_3F_6, and polymer, both in the absence and presence of NO. The results in the absence of NO are tabulated in Table VII. The C_2F_4 pressure was varied from 1.2 to 585 Torr, the SO_2 pressure from 2 to 500 Torr, and I_a from 0.0415 to 3.13 μ/sec. The variations of $\Phi\{CF_2O\}$ with C_2F_4 pressure are shown in Figure 4. For $[C_2F_4] > 30$ Torr, the results are scattered, but $\Phi\{CF_2O\} \sim 0.05$, independent of $[SO_2]$ and I_a. At lower C_2F_4 pressures, the results are more reliable, both because the background C_2F_4 peaks were smaller and because scale expansion of the infrared spectrum was employed. $\Phi\{CF_2O\}$ falls with $[C_2F_4]$, the values at higher $[SO_2]$ lying below those at lower $[SO_2]$. The addition of a large excess of N_2 had no effect on $\Phi\{CF_2O\}$.

The values for c-C_3F_6 are badly scattered, but $\Phi\{c\text{-}C_3F_6\}$ does increase with C_2F_4 pressure, and is not markedly affected by changes in SO_2 pressure. The addition of NO inhibits both CF_2O and c-C_3F_6 production. The effect on CF_2O is shown in Table VIII; $\Phi\{CF_2O\}$ drops as $[NO]/[C_2F_4]$ is enhanced.

Discussion

At the pressures of SO_2 used in this study (*i.e.*, ≥ 1 Torr), reactions 2 and 3 are unimportant[3,4,7] and the mechanism involving the emitting states reduces to

$$^1SO_2 + SO_2 \longrightarrow 2SO_2 \qquad (1a)$$

$$\longrightarrow {}^3SO_2 + SO_2 \qquad (1b)$$

$$^3SO_2 + SO_2 \longrightarrow 2SO_2 \qquad (4a)$$

$$\longrightarrow SO_3 + SO \qquad (4b)$$

The steady-state concentrations of the excited states are inversely proportional to $[SO_2]$. If these states reacted with CO or C_2F_4 to produce products, then the quantum yields of product formation should depend on the SO_2 pressure. This expectation has been confirmed for $^3SO_2$ by the results of Jackson and Calvert[24] in the SO_2–CO system.

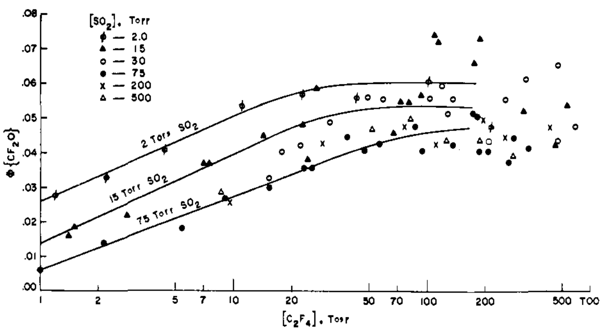

Figure 4. Semilog plots of $\Phi\{CF_2O\}$ *vs.* the C_2F_4 pressure at various SO_2 pressures in the photolysis of SO_2–C_2F_4 mixtures at 3130 Å and room temperature.

Our results, as well as those of Dainton and Ivin,[21] show that the product quantum yields are independent of SO_2 pressure at high SO_2 pressures. The addition of N_2, a known quencher of both SO_2 fluorescence and phosphorescence,[6] did not eliminate chemical reaction with either CO, C_2F_4, or n-C_4H_{10}. The results of Timmons[22] showed that excess CH_4, another known quencher of both SO_2 fluorescence and phosphorescence,[6] did not eliminate chemical reaction. Finally, some recent experiments of McQuigg and Allen[25] have shown that SO_2 is removed when irradiated at 3130 Å in the presence of O_2. The quantum yield of SO_2 disappearance was 7×10^{-3} independent of reactant pressures (20–400 Torr of O_2, 20–200 Torr of SO_2) or the addition of N_2 or CO_2.

It is clear that the electronic states predominantly involved in chemical reaction when SO_2 is irradiated at 3130 Å must be different from the emitting states. Furthermore, the results of the studies with added biacetyl or NO indicate two such states, one a singlet and the other a triplet.

It is apparent that the complete mechanism is complex. We shall propose as simplified a mechanism as possible to account for the observations. It should be realized that many possible steps will be omitted. Future work may alter the details of removal or even the order of formation of the excited states. For pure SO_2, the mechanism we envision is

$$SO_2 + h\nu(3130\ \text{Å}) \longrightarrow {}^1SO_2 \qquad \text{rate} = I_a$$

$$^1SO_2 + SO_2 \longrightarrow {}^3SO_2 + SO_2 \qquad (1b)$$

$$\longrightarrow SO_2{}^* + SO_2 \qquad (1c)$$

$$^3SO_2 + SO_2 \longrightarrow 2SO_2 \qquad (4a)$$

$$\longrightarrow SO_3 + SO \qquad (4b)$$

$$SO_2{}^* \longrightarrow SO_2{}^{**} \qquad (5)$$

$$SO_2{}^* + SO_2 \longrightarrow SO_2{}^{**} + SO_2 \qquad (6)$$

$$SO_2{}^{**} \longrightarrow SO_2 \qquad (7)$$

where $^1SO_2$ and $^3SO_2$ are respectively the singlet and triplet states which emit radiation, and $SO_2{}^*$ and $SO_2{}^{**}$ are respectively the singlet and triplet states which do not emit radiation. In the above mechanism, reaction 1a has been replaced by reaction 1c. Reactions 2 and 3 have been omitted, because they are unimportant at the SO_2 pressures used in our studies. The expanded

---

[25] R. D. McQuigg and E. R. Allen, 9th Informal Conference on Photochemistry, Columbus, Ohio, 1970.

Table VII. Photolysis of SO_2 in the Presence of C_2F_4 at 3130 Å and Room Temperature

$[C_2F_4]$, Torr	I_a, μ/sec	$10^2\Phi\{CF_2O\}$	$10^3\Phi\{c\text{-}C_3F_6\}$
$[SO_2]$ = 2.0 Torr			
1.2	0.175	2.80	
1.6[a]	0.170	2.64	
2.1[b]	0.170	1.52	
2.2	0.175	3.28	
4.3	0.175	4.08	
11.0	0.175	5.44	
22.4	0.175	5.67	
43.4	0.175	5.60	
100	0.170	6.10	
202	0.170	4.84	
$[SO_2]$ = 15 Torr			
1.4	0.97	1.65	
1.4[c]	0.97	1.54	
1.5	0.94	1.88	
1.5[d]	0.97	1.43	
2.8	1.09	2.23	
7.0	1.02	3.75	0.79
7.2	0.94	3.67	
14.2	1.09	4.45	
22.3	0.97	4.78	
22.3[e]	0.97	4.07	
22.3[f]	0.97	4.87	
24	0.110		5.36
24	1.35	3.82	1.54
26.5	0.94	5.90	
66	0.110	4.84	11.8
71.5	1.42	5.50	7.55
80	1.22	5.53	14.6
94.5	1.15	5.68	6.82
109	1.42	7.25	13.5
114	1.42	7.11	14.0
175.5	0.0415	6.58	19.7
184.5	1.15	7.36	23.2
228	1.15	8.12	30.4
316	1.02	5.33	41.2
484	1.02	4.47	45.6
524	1.42	5.44	
$[SO_2]$ = 30 Torr			
13	2.23	3.27	
17.5	2.27	4.05	
22	1.98	4.16	3.02
31	0.204	4.88	9.28
49	0.204	5.61	13.2
59	1.83	5.58	5.58
102	2.30	5.62	6.28
108	0.204	7.86	19.0
118	1.83	5.99	6.98
124	2.30	5.19	15.7
135	1.90	5.56	20.4
136	0.204	6.29	22.5
207	2.17	4.43	24.6
248	1.98	5.56	23.2
318	2.30	6.20	14.8
466	1.90	4.27	12.9
475	2.23	6.62	
585	2.30	4.84	
$[SO_2]$ = 75 Torr			
1.0	3.06	0.61	
2.2	2.80	1.23	
5.4	3.06	1.85	
9	3.13	2.69	
15.1	3.06	3.09	
23	3.02	3.63	
25.0	2.80	3.51	
32	0.298	3.63	4.26
38	3.02	4.48	4.90
47	0.298	4.13	4.39
56	0.298	4.31	6.30
56	3.02	3.99	5.15
86	3.02	4.79	4.75
94	0.298	4.07	15.1
124	0.298	3.53	8.02
137	3.02	4.34	6.90
170	3.13	5.17	9.23
179	3.02	5.08	16.5
184	3.16	4.12	13.6
204	2.97	4.06	15.2
258	3.02	3.77	14.0
276	3.02	4.47	12.2
330	3.13	4.24	20.5
478	2.97	4.45	26.0
$[SO_2]$ = 200 Torr			
9.5	2.82	2.57	
28.5	3.02	4.28	
75.5	2.94	4.83	2.84
110	3.02	4.28	5.48
189	3.10	5.04	6.53
252	3.02	4.51	12.3
423	2.94	4.77	13.6
$[SO_2]$ = 500 Torr			
8.5	2.82	2.89	
51	2.82	4.68	2.22
81	2.82	4.90	4.58
125	2.82	4.39	5.96
130	2.82	4.17	9.20
186	2.82	4.43	6.82
267	3.10	3.90	11.35

[a] 525 Torr of N_2 present. [b] 375 Torr of N_2 present. [c] 594 Torr of N_2 present. [d] 261 Torr of N_2 present. [e] 304 Torr of N_2 present. [f] 544 Torr of N_2 present.

mechanism does not alter the steady-state expressions for $[^1SO_2]$ or $[^3SO_2]$. Thus the rate laws for fluorescence and phosphorescence will be unchanged.

SO_2–CO System. With CO present, the additional reactions needed are

$$^1SO_2 + CO \longrightarrow SO_2^* + CO \qquad (8a)$$

$$\longrightarrow SO + CO_2 \qquad (8b)$$

$$SO_2^* + CO \longrightarrow SO + CO_2 \qquad (9)$$

$$SO_2^{**} + CO \longrightarrow SO + CO_2 \qquad (10)$$

$$^3SO_2 + CO \longrightarrow SO_2 + CO \qquad (11a)$$

$$\longrightarrow SO + CO_2 \qquad (11b)$$

The SO produced reacts on the wall to ultimately yield SO_2 and S_2, though S_2O is probably an intermediate. The ratio k_{11b}/k_{11} is about 0.1,[24] where $k_{11} \equiv k_{11a} + k_{11b}$. One important difference between the quenching of $^1SO_2$ by SO_2 and CO should be noted. When SO_2 removes $^1SO_2$, $^3SO_2$ is produced about 8% of the time.[7] However, CO must be very much less efficient than SO_2 in producing $^3SO_2$ to be consistent with both our findings and those of Jackson and Calvert. For simplicity, we have ignored the production of $^3SO_2$ by CO quenching of $^1SO_2$. Also, since the curves in Figure 3 continue to rise with [CO] and show no tendency to level off at high [CO], the quenching of SO_2^* and SO_2^{**} by CO is unimportant compared to other quenching processes.

The mechanism predicts that

$$\Phi\{CO_2\} = \Phi^1\{CO_2\} + \Phi^*\{CO_2\} + \Phi^{**}\{CO_2\} + \Phi^3\{CO_2\} \qquad (I)$$

Table VIII. Photolysis of SO_2 in the Presence of C_2F_4 and NO at 3130 Å and Room Temperature

[NO], Torr	$[C_2F_4]$, Torr	$\Phi\{CF_2O\}$
$[SO_2] = 15$ Torr, $I_a = 0.97\ \mu$/sec, $[C_2F_4] \sim 1.6$ Torr		
0.73	1.7	0.0083
5.2	1.6	~0.0018
20.8	1.6	~0.0014
$[SO_2] = 15$ Torr, $I_a = 0.97\ \mu$/sec, $[C_2F_4] \sim 22$ Torr		
1.2	23.3	0.037
4.8	22.1	0.0213
10.4	21.2	0.0160
24	22.3	0.0122
50	22.6	0.0086
76	22.9	0.0124
$[SO_2] = 30$ Torr, $I_a = 1.37\ \mu$/sec, $[C_2F_4] \sim 20$ Torr		
2.4	21.5	0.026
4.3	21	0.023
8.3	19.5	0.0145
$[SO_2] = 30$ Torr, $I_a = 1.46\ \mu$/sec, $[C_2F_4] \sim 36$ Torr		
6	38.5	0.025
13	35	0.0112
36	34	0.0078
40.5	38	0.0102
67	35	≤ 0.015
103.5	36.5	≤ 0.016
$[SO_2] = 30$ Torr, $I_a = 1.40\ \mu$/sec, $[C_2F_4] \sim 150$ Torr		
2	112	0.051
4.8	171	0.048
14	141.5	0.043
74	135	0.023
$[SO_2] = 75$ Torr, $I_a = 1.76\ \mu$/sec, $[C_2F_4] \sim 24$ Torr		
3.2	24.5	0.022
8	23.5	0.018
14	23	0.013
31	25	0.0064
65	27	≤ 0.0057

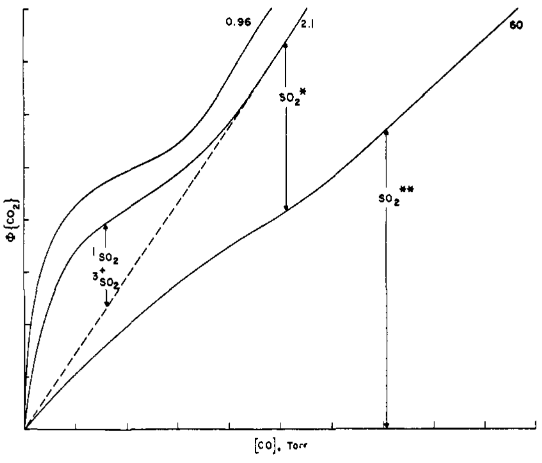

Figure 5. Expanded portion of the lower left-hand corner of Figure 3 showing the contributions of each of the excited electronic states. The numbers next to the lines refer to SO_2 pressures in Torr.

where the four terms on the right-hand side of eq I correspond to CO_2 production from the four excited electronic states of SO_2. The detailed expressions for the four terms are complex. However, with the realization that $k_9[CO]$ is always $\ll k_5 + k_6[SO_2]$, that $k_{1c}/k_1 = 0.92$, and that $k_{8a}/k_8 > 0.99$, the rate laws can be simplified by dropping $k_9[CO]$ in the appropriate places and setting $k_{1c}/k_1 = k_{8a}/k_8 = 1.0$. The resulting expressions for the individual terms become

$$\Phi^1\{CO_2\} \simeq k_{8b}[CO]/(k_1[SO_2] + k_8[CO]) \qquad \text{(II)}$$

$$\Phi^*\{CO_2\} \simeq k_9[CO]/(k_5 + k_6[SO_2]) \qquad \text{(III)}$$

$$\Phi^{**}\{CO_2\} \simeq k_{10}[CO]/k_7 \qquad \text{(IV)}$$

$$\Phi^3\{CO_2\} \simeq \frac{k_{1b}k_{11b}[CO][SO_2]}{(k_1[SO_2] + k_8[CO])(k_4[SO_2] + k_{11}[CO])} \qquad \text{(V)}$$

Before quantitatively analyzing the results, it is useful to qualitatively assess which terms are important for various experimental conditions. Portions of the lower part of Figure 3 are reproduced in Figure 5 for this purpose. At large SO_2 pressures, $\Phi^*\{CO_2\}$ is negligible. The principal contribution to $\Phi\{CO_2\}$ comes from $\Phi^{**}\{CO_2\}$, and this explains why $\Phi\{CO_2\}$ is proportional to [CO] but independent of $[SO_2]$ or I_a. Actually, there is also a contribution from both $\Phi^1\{CO_2\}$ and $\Phi^3\{CO_2\}$. (These contributions are not shown in Figure 5.) At high CO pressures, $\Phi^*\{CO_2\}$ becomes more important as $[SO_2]$ is reduced. This accounts for the enhancement in $\Phi\{CO_2\}$ at low SO_2 pressures. When both the SO_2 and CO pressures are low, all four terms are important, and this accounts for the bump on the curves.

Table IX. Summary of Rate Constant Data

Ratio	Value	Units	M	Source
k_{1b}/k_1	0.082	None		Ref 7
k_8/k_1	0.35	None		Ref 6
k_{11}/k_4	0.22	None		Ref 24
k_{11b}/k_{11}	0.066	None		Ref 24
k_{8b}/k_8	1.4×10^{-3}	None		Table III, eq II
k_7/k_{10}	8.0×10^4	Torr		Eq V, VI, Figure 6
k_{12}/k_7	0.0068	$Torr^{-1}$	O_2	Eq V, VI, Figure 6
k_{12}/k_7	1.0	$Torr^{-1}$	BiA	Eq V, VI, Figure 6
k_{12}/k_7	2.9	$Torr^{-1}$	NO	Eq V, VI, Figure 6
k_5/k_9	4×10^4	Torr		Eq VII, Figure 7
k_6/k_9	8.8×10^3	None		Eq VII, Figure 7
k_{16b}/k_7	6.1×10^{-3}	$Torr^{-1}$		$\Phi\{CF_2O\}$ for $[SO_2] = 75$ Torr, $[C_2F_4] = 1$ Torr
k_{15}/k_{15b}	72	None		Eq XII, Figure 10 ($[SO_2] = 15$ Torr)
k_5/k_{15b}	16	Torr		Eq XII, Figure 10
k_6/k_{15b}	4.6	None		Eq XII, Figure 10
k_{16}/k_{16b}	17	None		Eq XIII, Figure 11
k_{12}/k_{16b}	404	None		Eq XIII, Figure 11

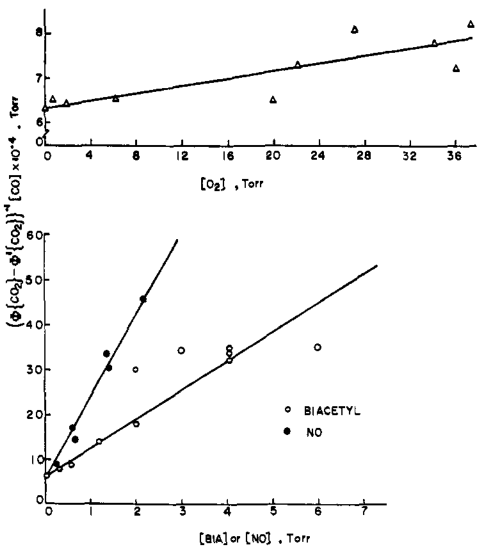

Figure 6. Plots of $(\Phi\{CO_2\} - \Phi^1\{CO_2\})^{-1}[CO]$ *vs.* [M] (M = NO, BiA, or O_2) in the photolysis of SO_2–CO–M mixtures at 3130 Å and room temperature. $\Phi^1\{CO_2\}$ is computed from eq II and the rate constant ratios listed in Table IX.

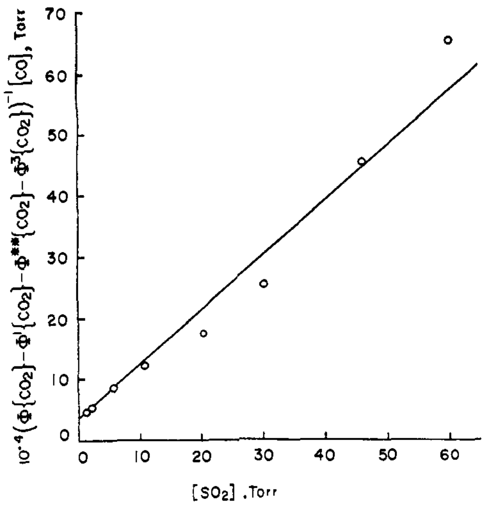

Figure 7. Plot of $(\Phi\{CO_2\} - \Phi^1\{CO_2\} - \Phi^{**}\{CO\}_2 - \Phi^3\{CO_2\})^{-1}\cdot[CO]$ *vs.* SO_2 pressure in the photolysis of SO_2–CO mixtures at 300 Torr of CO, 3130 Å, and room temperature. Values for $\Phi\{CO_2\}$ are taken from curves of Figure 3 at 300 Torr of CO for each SO_2 pressure. Values for $\Phi^1\{CO_2\}$, $\Phi^{**}\{CO_2\}$, and $\Phi^3\{CO_2\}$ are computed from eq II, IV, and V, respectively, and the rate constant ratios listed in Table IX.

The quantitative importance of $\Phi^3\{CO_2\}$ can be computed from the rate constants reported by Mettee[6] and by Calvert and his coworkers.[7,24] Values of the appropriate rate constant ratios are listed in Table IX. The maximum value for $\Phi^3\{CO_2\}$ of 1.06×10^{-3} occurs when $[SO_2]/[CO] = (k_8k_{11}/k_1k_4)^{1/2} = 0.28$. This term is never dominant, but it can account for about 20% of $\Phi\{CO_2\}$ at CO pressures below about 100 Torr.

At high SO_2 pressures, the contribution of $\Phi^*\{CO_2\}$ is negligible. The contributions of $\Phi^1\{CO_2\}$ can be evaluated by adding triplet quenchers

$$SO_2^{**} + M \longrightarrow SO_2 + M \qquad (12)$$

$$^3SO_2 + M \longrightarrow SO_2 + M \qquad (13)$$

where M is biacetyl (BiA), NO, or O_2. With about 400 Torr of CO and high pressures of SO_2, the data in Tables II and III show that $\Phi\{CO_2\}$ can be reduced by the addition of BiA or NO to about 1.0×10^{-3}. This value corresponds to the right-hand side of eq II. By fitting the extrapolated values in Table III for very high NO pressures, and using $k_8/k_1 = 0.35$,[6] we find $k_{8b}/k_8 = 1.4 \times 10^{-3}$.

The quenching constants of the triplet quenchers can be found from the results at lower quencher pressures. Ignoring the minor contributions of $\Phi^*\{CO_2\}$ and $\Phi^3\{CO_2\}$ at high SO_2 pressures, the mechanism predicts that

$$(\Phi\{CO_2\} - \Phi^1\{CO_2\})^{-1}[CO] = k_7/k_{10} + k_{12}[M]/k_{10} \qquad (VI)$$

$\Phi^1\{CO_2\}$, and thus the left-hand side of eq VI, can be computed. The values so obtained are plotted *vs.* the quencher gas pressure in Figure 6. For all three cases the plots yield reasonable straight lines. The intercepts, which are computed from runs in the absence of the quenching gas, should give k_7/k_{10}, and the ratio of slope to intercept should yield k_{12}/k_7. In fact, the contribution of $\Phi^3\{CO_2\}$ is fairly significant, so that eq VI is an oversimplification. The values of k_{12}/k_7 so obtained are listed in Table IX, but they really represent some composite quenching constant of the two triplet states, though the dominant state is SO_2^{**}. From these results, the relative quenching constant for NO and O_2 is 420 compared to the value of 173 found for $^3SO_2$ by Mettee.[6] Also, the relative quenching constant for BiA and O_2 is about 150, compared to the value of 158–845 estimated from the results of Rao, *et al.*,[7,8] (also for quenching of both $^3SO_2$ and SO_2^{**}, though probably in different proportions). The intercept value of 6.3 can be used to compute k_7/k_{10} if the correction from $\Phi^3\{CO_2\}$ (computed from eq V) is made. When this is done k_7/k_{10} is computed to be 8.0×10^4 Torr.

At high CO pressures, the contribution of $\Phi^3\{CO_2\}$ drops to zero but $\Phi^*\{CO_2\}$ becomes important as the SO_2 pressure is reduced. The mechanism predicts that

$$(\Phi\{CO_2\} - \Phi^1\{CO_2\} - \Phi^{**}\{CO_2\} - \Phi^3\{CO_2\})^{-1}[CO] = k_5/k_9 + k_6[SO_2]/k_9 \qquad (VII)$$

Values for $\Phi\{CO_2\}$ at 300 Torr of CO and various values of $[SO_2]$ are taken from the curves of Figure 3. The other quantum yields can be evaluated at 300 Torr of CO from eq II, IV, and V and the rate constant ratios in Table IX. Thus values of the left-hand side of eq VII can be computed. They are plotted *vs.* $[SO_2]$ in Figure 7, and the points lie on a line. The intercept yields $k_5/k_9 = 4 \times 10^4$ Torr and the slope gives $k_6/k_9 = 8.8 \times 10^3$.

Now all the pertinent rate constant ratios have been obtained. If the mechanism is consistent, then it should be possible to compute $\Phi\{CO_2\}$ from the rate constant ratios and reproduce the data points. The solid curves in Figure 8 are the theoretically computed values of $\Phi\{CO_2\}$ at 2.1 and 60 Torr of SO_2. They fit the data points reasonably well.

A further check of the consistency of the mechanism can be made by adding 6 Torr (or more) of NO to remove the triplet states or by adding excess N_2 to remove the emitting states, since N_2 should act like CO and quench $^1SO_2$ to SO_2^*. The results of these experiments for 2.1 Torr of SO_2 are in Table VI. Based on these results, computed values of $\Phi^1\{CO_2\} + \Phi^*$-

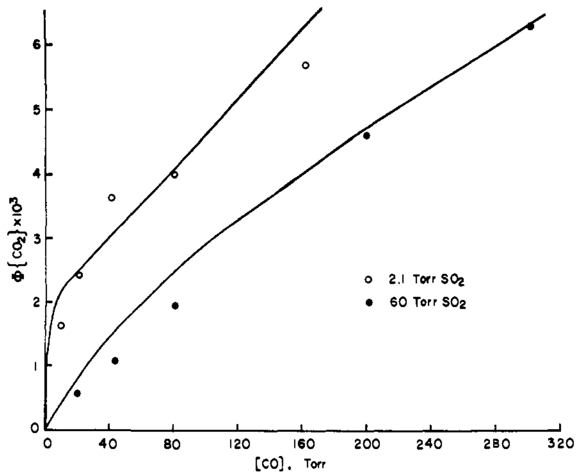

Figure 8. Plots of $\Phi\{CO_2\}$ *vs.* [CO] in the photolysis of SO_2–CO mixtures at 3130 Å and room temperature at 2.1 and 60 Torr of SO_2. The data points are from Table V. The solid lines are the theoretical curves for $\Phi\{CO_2\}$ at 2.1 Torr of SO_2 (upper curve) and 60 Torr of SO_2 (lower curve) computed from eq I–V and the rate constant ratios in Table IX.

$\{CO_2\}$ and $\Phi^*\{CO_2\} + \Phi^{**}\{CO_2\}$ can be compared to the observed values. This is done in Table X. In all cases the agreement between the observed and computed values is good.

Table X. Comparison of Observed and Computed Quantum Yields of CO_2 Formation at 2.1 Torr of SO_2

[CO], Torr	$10^3\Phi\{CO_2\}$ Obsd[a]	$10^3\Phi\{CO_2\}$ Comp	$10^3(\Phi^1\{CO_2\} + \Phi^*\{CO_2\})$ Obsd[b]	$10^3(\Phi^1\{CO_2\} + \Phi^*\{CO_2\})$ Comp	$10^3(\Phi^*\{CO_2\} + \Phi^{**}\{CO_2\})$ Obsd[c]	$10^3(\Phi^*\{CO_2\} + \Phi^{**}\{CO_2\})$ Comp
~45	3.6	3.1	1.9	2.0	1.6	1.3
~84	4.0	4.1	2.6	2.7		2.5
~170	5.6	6.5	4.4	4.2		5.0
~300	10.1	10.4	5.8	6.5	10.6	8.9
391	15.0	13.1	9.2	8.0		11.6

[a] $\Phi\{CO_2\}$ in the absence of N_2 and NO. [b] $\Phi\{CO_2\}$ in the presence of >6 Torr of NO. [c] $\Phi\{CO_2\}$ in the presence of excess N_2.

SO_2–C_2F_4 System. The results in the SO_2–C_2F_4 system show that N_2 does not inhibit CF_2O production. Therefore, the emitting states, which are strongly quenched by N_2, are not chemically important. On the other hand, C_2F_4 is an efficient quencher of both SO_2^* and SO_2^{**}, since $\Phi\{CF_2O\}$ approaches a constant value at high $[C_2F_4]$. The additional reactions that are needed are

$$^1SO_2 + C_2F_4 \longrightarrow SO_2^* + C_2F_4 \quad (14)$$

$$SO_2^* + C_2F_4 \longrightarrow SO_2^{**} + C_2F_4 \quad (15a)$$

$$\longrightarrow SO + CF_2O + CF_2 \quad (15b)$$

$$SO_2^{**} + C_2F_4 \longrightarrow SO_2 + C_2F_4 \quad (16a)$$

$$\longrightarrow SO + CF_2O + CF_2 \quad (16b)$$

The SO species is converted to SO_2 and S_2 on the cell wall. CF_2 can either dimerize or add to C_2F_4 to produce $c\text{-}C_3F_6$

$$2CF_2 \longrightarrow C_2F_4 \quad (17)$$

$$CF_2 + C_2F_4 \longrightarrow c\text{-}C_3F_6 \quad (18)$$

Since CF_2 is removed mainly by reaction 17, the mechanism predicts that

$$\Phi\{c\text{-}C_3F_6\} = k_{18}[C_2F_4](\Phi\{CF_2O\}/2k_{17}I_a)^{1/2} \quad \text{(VIII)}$$

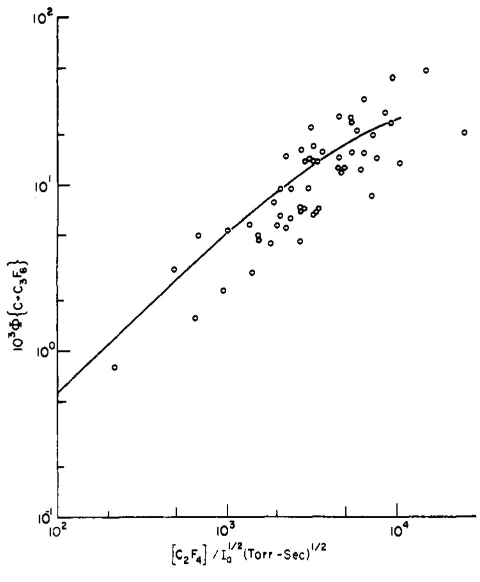

Figure 9. Plot of $\Phi\{c\text{-}C_3F_6\}$ *vs.* $[C_2F_4]/I_a^{1/2}$ in the photolysis of SO_2–C_2F_4 mixtures at 3130 Å and room temperature. The solid line is the theoretical value based on $k_{18}/k_{12}^{1/2} = 3.63 \times 10^{-5}$ (Torr sec)$^{-1/2}$ and $\Phi\{CF_2O\} = 0.050$.

The ratio $k_{18}/k_{17}^{1/2}$ is known to be 3.63×10^{-5} (Torr sec)$^{-1/2}$ at room temperature.[26] $\Phi\{c\text{-}C_3F_6\}$ could only be measured at high C_2F_4 pressures where $\Phi\{CF_2O\} \simeq 0.05$. Thus theoretical values of $\Phi\{c\text{-}C_3F_6\}$ can be computed for any value of $[C_2F_4]/I_a^{1/2}$ using these values for $k_{18}/k_{17}^{1/2}$ and $\Phi\{CF_2O\}$. This computation has been done, and the results are given by the solid line in Figure 9. The experimental values of $\Phi\{c\text{-}C_3F_6\}$ obtained in this study are also plotted on the same figure. The data points are scattered badly about the theoretical line, but they are consistent with the above interpretation.

The quantum yield of CF_2O production can be split into its component parts

$$\Phi\{CF_2O\} = \Phi^*\{CF_2O\} + \Phi^{**}\{CF_2O\} \quad \text{(IX)}$$

where $\Phi^*\{CF_2O\}$ and $\Phi^{**}\{CF_2O\}$ are respectively the contribution to $\Phi\{CF_2O\}$ from SO_2^* and SO_2^{**}. In the absence of triplet quenchers, the mechanism predicts the following rate law for the individual terms

$$\Phi^*\{CF_2O\} = k_{15b}[C_2F_4]/(k_5 + k_6[SO_2] + k_{15}[C_2F_4]) \quad \text{(X)}$$

$$\Phi^{**}\{CF_2O\} = k_{16b}[C_2F_4]/(k_7 + k_{16}[C_2F_4]) \quad \text{(XI)}$$

For large values of $[SO_2]/[C_2F_4]$, the contribution of $\Phi^*\{CF_2O\}$ is small and can be neglected. Furthermore, at very low C_2F_4 pressures, $k_{16}[C_2F_4] \ll k_7$, so that $\Phi\{CF_2O\} \simeq k_{16b}[C_2F_4]/k_7$. From the value of $\Phi\{CF_2O\}$ at 75 Torr of SO_2 and 1 Torr of C_2F_4, k_{16b}/k_7 can be estimated to be 6.1×10^{-3} Torr^{-1}.

The mechanism further predicts that

$$(\Phi\{CF_2O\} - \Phi^{**}\{CF_2O\})^{-1}[C_2F_4] = (k_5 + k_6[SO_2] + k_{15}[C_2F_4])/k_{15b} \quad \text{(XII)}$$

For low C_2F_4 pressures, $\Phi^{**}\{CF_2O\}$ can be taken to be $\Phi\{CF_2O\}$ at 75 Torr of SO_2; the left-hand side of eq XII can be computed. At any SO_2 pressure, a

(26) N. Cohen and J. Heicklen, *J. Chem. Phys.*, **43**, 871 (1965).

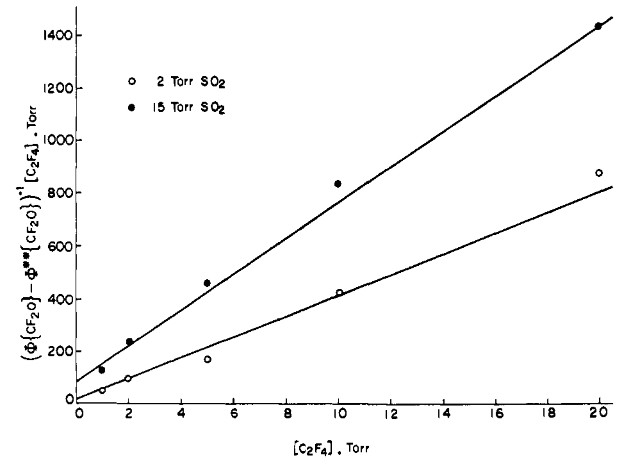

Figure 10. Plots of $(\Phi\{CF_2O\} - \Phi^{**}\{CF_2O\})^{-1}[C_2F_4]$ *vs.* C_2F_4 pressure at 2 and 15 Torr of SO_2 in the photolysis of SO_2–C_2F_4 mixtures at 3130 Å and room temperature. Values of $\Phi\{CF_2O\}$ are taken from the curves of Figure 4. Values of $\Phi^{**}\{CF_2O\}$ are taken from curve of Figure 4 for $[SO_2] = 75$ Torr.

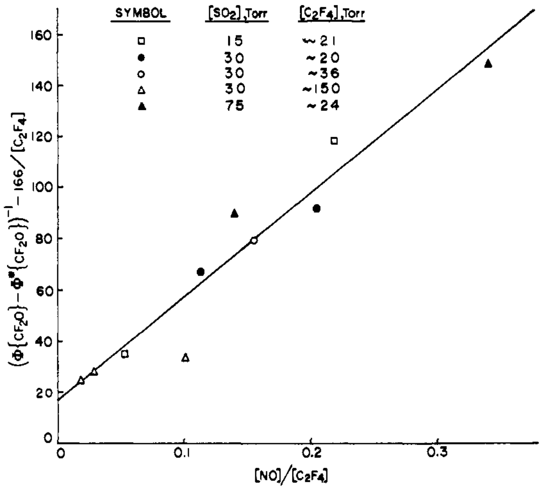

Figure 11. Plot of $(\Phi\{CF_2O\} - \Phi^{*}\{CF_2O\})^{-1} - 166/[C_2F_4]$ *vs.* $[NO]/[C_2F_4]$ in the photolysis of SO_2–C_2F_4–NO mixtures at 3130 Å and room temperature. In computing the ordinate, $\Phi^{*}\{CF_2O\} = [C_2F_4]/(16 + 4.6[SO_2] + 72[C_2F_4])$, and all pressures are in Torr.

plot of the left-hand side of eq XII *vs.* $[C_2F_4]$ should yield a straight line. Such plots for 2 and 15 Torr of SO_2 are shown in Figure 10. At both SO_2 pressures, good straight lines are obtained. Actually the points on the graph give a better fit than warranted from the experimental results, because the values for $\Phi\{CF_2O\}$ used in the computations were taken from the smooth curves in Figure 4. The mechanism predicts that the slopes of both lines should be the same, whereas they are not. At 2 Torr of SO_2, the slope is 44, whereas at 15 Torr of SO_2, the slope is 72. This apparent discrepancy is not outside the experimental uncertainty, since the ordinate is computed as a difference of two similar numbers. Therefore, the exact placing of the curves in Figure 4 has a pronounced effect on Figure 10. The slope at 15 Torr of SO_2 gives a value for k_{15}/k_{15b} which is more consistent with the rest of the results and is adopted here. The intercepts of the two lines are approximately 25 and 85 Torr at 2 and 15 Torr of SO_2, respectively. From these values k_5/k_{15b} and k_6/k_{15b} can be estimated to be 16 Torr and 4.6, respectively. These values give $k_5/k_6 \simeq 3.5$ Torr, which compares favorably with the value of $\simeq$4.5 Torr estimated from the SO_2–CO system.

In the presence of NO, the mechanism predicts

$$(\Phi\{CF_2O\} - \Phi^{*}\{CF_2O\})^{-1} - k_7/k_{16b}[C_2F_4] = k_{16}/k_{16b} + k_{12}[NO]/k_{16b}[C_2F_4] \quad \text{(XIII)}$$

The value for k_7/k_{16b} has previously been estimated to be 166 Torr, so that the left-hand side of eq XIII can be computed. It is plotted *vs.* $[NO]/[C_2F_4]$ in Figure 11. A good straight line results whose intercept and slope yield values of $k_{16}/k_{16b} = 17$ and $k_{12}/k_{16b} = 404$, respectively. Combination of the rate constant ratios k_7/k_{16b} and k_{12}/k_{16b} yields $k_{12}/k_7 = 2.5$, which agrees well with the value of 2.9 found in the SO_2–CO system.

Correlation with Spectroscopy. It is now necessary to relate the four photochemical states of SO_2 with the known spectroscopic states. The lowest excited state of SO_2 is generally agreed to be $^3B_1$. This state is responsible for the weak absorption at 3900–3400 Å.[27] It is also the state which phosphoresces and is therefore the state designated $^3SO_2$. The second absorption band at 3400–2600 Å is much stronger and is probably that of the corresponding singlet state, $^1B_1$. Therefore, we assign the absorption at 3130 Å to the $^1B_1$ state, which is also the state which fluoresces, $^1SO_2$.

One difficulty in the SO_2 system is that the fluorescent lifetime of the excited singlet state is about 100 times greater than that computed from the integrated absorption coefficient.[1,3] This anomaly has been discussed by Douglas,[28] and he has ascribed the main effect to the mixing of the vibrational levels of the absorbing state with those of other electronic states. Walsh[29] has suggested that an optically forbidden $^1A_2$ state should exist. Such a state has been observed in the electronically similar NO_2^- ion.[30] We suggest that this state lies near the $^1B_1$ state. Furthermore, we propose that the $^1B_1$ and $^1A_2$ states are strongly coupled, and that collisional quenching of the $^1B_1$ state ($^1SO_2$) produces the $^1A_2$ state (SO_2^*).

The $^1A_2$ state should have a triplet state, $^3A_2$, which can be formed by intersystem crossing. Brand[31] has suggested that another triplet state lies about 2.5–3 kcal/mol above $^3B_1$. This would be SO_2^{**}, which could be the $^3A_2$ state.

Acknowledgment. We wish to thank Drs. Silvia Braslavsky, Jack Calvert, Howard Mettee, Stewart Strickler, and Howard Sidebottom for helpful discussions and useful suggestions. Correspondence with Drs. R. N. Dixon and John Brand was also beneficial. We appreciate the opportunity of having seen the results of Timmons, Jackson and Calvert, and Brand before publication. This work was supported by the National Air Pollution Control Administration under Grant No. AP-00022, for which we are grateful.

---

(27) G. Herzberg, "Electronic Spectra of Polyatomic Molecules," Van Nostrand, Princeton, N. J., 1966, pp 511–513.

(28) A. E. Douglas, *J. Chem. Phys.*, **45**, 1007 (1966).

(29) A. D. Walsh, *J. Chem. Soc.*, 2266 (1953).

(30) S. J. Strickler and M. Kasha, *J. Amer. Chem. Soc.*, **85**, 2899 (1963).

(31) J. C. D. Brand, private communication, 1970.